Analytic bond-order potentials beyond Tersoff-Brenner. II. Application to the hydrocarbons

I. I. Oleinik and D. G. Pettifor
Department of Materials, University of Oxford, Parks Road, Oxford OX1 3PH, United Kingdom

(Received 26 October 1998)

The accuracy of the analytic bond-order potentials (BOP's) that were derived in the previous paper within the tight-binding (TB) formalism is studied for the case of diamond, graphite, and the hydrocarbon molecules. The simplified four-level variant, BOP4S, is found to reproduce the TB bond orders of the C-H and C-C σ bonds to better than 6% due partly to the inclusion of the shape parameter $(b_2/b_1)^2$. The two-level matrix-derived expression BOP2M is shown to provide a good description of the saturated and conjugate π bonds, thereby overcoming the deficiencies of the Tersoff potential that are associated with overbinding of radicals and poor treatment of conjugacy. The analytic BOP's reproduce the C-H and C-C bond energies to better than 0.9 eV per bond. The errors would be reduced if the analytic potentials were fitted to experiment rather than predicted directly from known TB parameters. [S0163-1829(99)02813-1]

I. INTRODUCTION

The hydrocarbons provide an ideal system for testing the analytic bond-order potentials (BOP's) derived in the previous paper,[1] since the tight-binding (TB) model upon which they are based has already been shown to provide a good treatment of their energetics.[2] Moreover, the hydrocarbons are a system that Brenner[3] found was very poorly described by the original form of the Tersoff potential[4] due to its inherent overbinding of radicals and incorrect handling of conjugation. These drawbacks led Brenner to introduce a further twenty-three parameters, F_{ij} and H_{ij}, in order to fit the energetics of the individual C-C and C-H bonds within the hydrocarbons. It is hoped that the inclusion of an explicit π bond contribution within the analytic BOP's will help to avoid the shortcomings of the Tersoff potential and the *ad hoc* nature of the extra terms in the Brenner potential.

In this paper, therefore, we examine how reliably the analytic BOP's model the energetics of the σ and π bonds in diamond, graphite, and the hydrocarbons. In Sec. II we present the TB parametrization[2,5,6] for the C-C and C-H bond integrals that we use in later sections. In Sec. III we compare the σ and π bond orders predicted by the analytic BOP's with the TB values obtained by matrix diagonalization. We will see that the BOP's provide a quantification of the ubiquitous valence bond concept of single, double, triple, and conjugate bonds between carbon atoms. In Sec. IV we compare the total binding energies predicted by the analytic BOP's with the exact TB values. We will find that the analytic BOPs reproduce the tight-binding C-H and C-C bond energies to an accuracy of better than 0.9 eV per bond. This error is comparable with that between the original TB model and experiment.[2] In Sec. V we conclude.

II. THE TIGHT-BINDING PARAMETRIZATION

We saw in the previous paper[1] that our TB model approximates the binding energy of a carbon-hydrogen system by the sum of three terms, namely

$$U = U_{rep} + U_{prom} + U_{bond}, \tag{1}$$

where the parameters characterizing the first term are given in Tables I and II of Ref. 2. The second term, the promotion energy, depends on the splitting between the s and p energy levels in carbon, which takes the value $\delta = E_p^C - E_s^C = 6.7$ eV.[5] The third term, U_{bond}, can be decomposed in terms of the individual bond energies $(U_{bond})_{ij}^{\mu\nu}$ between an atomic species μ on site i and an atomic species ν on site j. It may be expressed as the product of the bond integrals and the bond orders as

$$(U_{bond})_{ij}^{\mu\nu} = -2\Theta_{ij,\sigma}^{\mu\nu} h_{\sigma}^{\mu\nu}(R_{ij}) - 2(\Theta_{ij,\pi_x}^{\mu\nu} + \Theta_{ij,\pi_y}^{\mu\nu}) h_{\pi}^{\mu\nu}(R_{ij}) \delta_{\mu C}\delta_{\nu C}. \tag{2}$$

The TB parametrization for the C-C and C-H bond integrals has been assumed[5,6] to take the Goodwin, Skinner, and Pettifor (GSP) form,[7] namely

$$h_{\tau}^{\mu\nu}(R) = h_{\tau}^{\mu\nu}(R_0)\left(\frac{R_0}{R}\right)^n \exp\left\{ n\left[-\left(\frac{R}{R_c}\right)^{n_c} + \left(\frac{R_0}{R_c}\right)^{n_c} \right]\right\}, \tag{3}$$

TABLE I. Comparison of TB binding energies (energies in eV/molecule except graphite and diamond which are in eV/atom).

System	Conventional TB	Reduced TB	Experiment
C_2	−4.04	−4.74	−6.34
C_{gr}	−7.25	−7.36	−7.38
$C_{\diamond}$	−7.23	−7.23	−7.35
CH_3	−12.51	−12.50	−12.7
CH_4	−17.59	−17.59	−17.6
C_2H_2	−16.14	−16.31	−17.1
C_2H_4	−23.61	−23.70	−23.6
C_2H_5	−25.07	−25.11	−25.5
C_2H_6	−29.98	−29.99	−29.7
C_6H_6	−57.61	−58.15	−57.5
C_6H_{12}	−74.37	−74.37	−73.6

TABLE II. C-H σ bond orders.

System	z	R_0^{CH} (Å)	h_σ^{CH} (eV)	$\hat{b}_1$ BOP4S BOP4Z	$\hat{b}_2$ BOP4S BOP4Z	$\hat{b}_3$ BOP4S BOP4Z	$(b_2/b_1)^2$ BOP4S BOP4Z	Θ_σ^{CH} BOP2S	Θ_σ^{CH} BOP4S	Θ_σ^{CH} BOP4Z TBZ	Θ_σ^{CH} BOP4 TB
C_2H_2	2	1.060	9.818	1.002	0.145	1.002	0.021	0.998	1.003	1.000	0.992
				1.002	0.145	1.953	0.021			1.000	0.993
CH_3	3	1.080	9.491	1.023	0.308	1.023	0.091	0.978	0.990	0.989	0.977
				1.023	0.308	1.036	0.091			0.989	0.977
C_2H_4	3	1.087	9.377	1.039	0.489	1.039	0.221	0.962	1.006	0.981	0.960
				1.045	0.503	1.427	0.232			0.982	0.973
$C_2H_5^{(1)}$	3	1.076	9.556	1.026	0.344	1.026	0.112	0.974	0.991	0.986	0.943
				1.029	0.361	1.159	0.123			0.986	0.975
C_6H_6	3	1.086	9.393	1.046	0.544	1.046	0.270	0.956	1.010	0.977	0.953
				1.056	0.559	1.394	0.281			0.979	0.963
CH_4	4	1.087	9.377	1.066	0.544	1.066	0.261	0.938	0.973	0.972	0.962
				1.066	0.544	1.082	0.261			0.972	0.962
$C_2H_5^{(2)}$	4	1.086	9.393	1.075	0.592	1.075	0.303	0.930	0.973	0.965	0.951
				1.078	0.598	1.124	0.307			0.964	0.956
$C_2H_5^{(3)}$	4	1.090	9.328	1.077	0.602	1.077	0.312	0.928	0.972	0.963	0.948
				1.080	0.604	1.133	0.312			0.956	0.947
C_2H_6	4	1.094	9.263	1.074	0.588	1.074	0.299	0.931	0.973	0.965	0.942
				1.077	0.599	1.156	0.309			0.967	0.958
$C_6H_{12}^{(1)}$	4	1.103	9.118	1.076	0.601	1.076	0.312	0.929	0.974	0.962	0.927
				1.082	0.626	1.204	0.334			0.964	0.955
$C_6H_{12}^{(2)}$	4	1.106	9.078	1.080	0.616	1.080	0.325	0.926	0.971	0.960	0.921
				1.087	0.642	1.214	0.349			0.962	0.954

where $\tau=\sigma$ or π and $R_0\equiv R_0^{\mu\nu}$ with R_0^{CC} and R_0^{CH} the equilibrium bond lengths for diamond ($R_0^{CC}=1.5363$ Å) and methane ($R_0^{CH}=1.084$ Å), respectively. The other fitting parameters $n\equiv n^{\mu\nu}$, $n_c\equiv n_c^{\mu\nu}$, and $R_c\equiv R_c^{\mu\nu}$ are given in Table II of Ref. 2 together with two further parameters which guarantee that the tail of the bond integral vanishes smoothly at some cutoff distance $R_{cut}(R_{cut}^{CC}=2.60$ Å, $R_{cut}^{CH}=1.85$ Å). In this paper, however, we have chosen R_{cut}^{CC} to be 2.40 Å rather than 2.60 Å in order to guarantee that the second-nearest-neighbor interactions in benzene are zero.

The values of the bond integrals at the distance R_0 are determined by the prefactor $h_\tau^{\mu\nu}(R_0)$ in Eq. (3). We saw in Eq. (6) of Paper I that the *three* independent C-C bond integrals $ss\sigma^{CC}$, $sp\sigma^{CC}$, and $pp\sigma^{CC}$ have been reduced to the *two* independent variables $p_\sigma=pp\sigma^{CC}/|ss\sigma|^{CC}$ and h_σ^{CC} in order to compact the usual TB expression for the σ bond energy to a single term as in Eq. (2). The variable p_σ controls the angular function $g_\sigma(\theta)$ [see Eq. (82) of Paper I] and takes the value $p_\sigma=1.100$ for Xu *et al's*[5] set of carbon TB parameters. We fix the other variable h_σ^{CC} by requiring that it leads to the same bond energy for equilibrium diamond as the original TB fit.[5] We find $h_\sigma^{CC}(R_0^{CC})=10.016$ eV which is six times larger than the π bond integral, $h_\pi^{CC}(R_0^{CC})=1.550$ eV[5]. Further, we saw from Eq. (8) of Paper I that the *two* independent C-H bond integrals $ss\sigma^{CH}$ and $sp\sigma^{CH}$ have been reduced to the *single* independent variable h_σ^{CH}, once p_σ has been determined by the ratio of the two appropriate C-C bond integrals. This was in order to characterize the angular function $g_\sigma^C(\theta)$ by a single function that was independent of whether we had C-C or C-H bonding. We, therefore, fix the value of h_σ^{CH} by requiring that it leads to the same σ bond energy of methane at its equilibrium geometry as the original TB fit.[2,6] We find $h_\sigma^{CH}(R_0^{CH})=9.453$ eV.

The errors made by reducing the number of independent C-C and C-H integrals within the conventional two-center TB scheme[8] are small for carbon and the hydrocarbons since $sp\sigma^{CC}/ss\sigma^{CC}$ and $(|pp\sigma^{CC}|/ss\sigma^{CC})^{1/2}$ agree to within 12% (Ref. 5) and $sp\sigma^{CH}/ss\sigma^{CH}$ equals $sp\sigma^{CC}/ss\sigma^{CC}$ to within 0.4%.[6] This is reflected in Table I where the binding energy predicted by the reduced TB scheme[1] is compared with those predicted by the conventional TB scheme.[2] The bond lengths and the bond angles have been fixed at the experimental equilibrium values and the dimer C_2 has been chosen with the experimental ground-state configuration $\sigma_g^2\sigma_u^2\pi_u^4$. We see that the errors are indeed small. The C-H bond in the methyl radical shows the negligible error of 0.003 eV/bond, whereas that in the methane molecule is exact since it was used as a reference in the fitting of $h_\sigma^{CH}(R_0^{CH})$. The C-C single bonds show errors of less than 0.01 eV/bond for C_2H_6 and C_6H_{12}, whereas that in diamond is exact through the fitting of $h_\sigma^{CC}(R_0^{CC})$. The C-C double bond in C_2H_4 shows an error of 0.09 eV/bond, whereas the C-C triple bonds in C_2 and C_2H_2 show errors of 0.7 eV/bond and 0.17 eV/bond, respectively. The parameters for the C-C interactions within the conventional TB scheme[2] have been fitted to guarantee that graphite is slightly more stable than diamond. A small increase in the relative hardness[9] of the repulsive pairwise potential $\phi^{CC}(R)$ would decrease the current graphite-diamond energy difference of 0.13 eV/atom within the reduced TB scheme to closer the experimental difference of 0.03 eV/atom.

Table I also gives the experimental values of the binding energies, which have been derived from the heats of formation without any zero-point energy corrections.[4] We see that the conventional TB scheme[2] reproduces these values extremely well apart from the triple-bonded systems C_2 and C_2H_2 where the errors are 1.7 eV and 1.0 eV, respectively. This discrepancy is probably due to the GSP approximation[7] of taking the σ and π bond integrals to display the same distance dependence. This causes the π bond integral in the dimer to be smaller than expected, thereby reducing the magnitude of the TB binding energy. Moreover, it leads to the prediction of the wrong ground state for C_2, namely $\sigma_g^2\sigma_u^2\sigma_g^2\pi_u^2$ rather than $\sigma_g^2\sigma_u^2\pi_u^4$. The analytic BOP formalism, therefore, relaxes this GSP constraint and assumes in general that the distance dependencies of the h_σ and h_π integrals are different (although in this paper we retain the GSP fit for comparison purposes). Finally, we should note that the radicals CH and CH_2 have not been considered here because the TB model[2] predicts these radicals to take the wrong ground-state configuration due to the neglect of spin polarization. Their correct treatment would require extending the TB model to include spin polarization as, for example, in Secs. 3.4 and 8.6 of Ref. 9.

III. BOND ORDERS

In this section we compare the bond orders predicted by the analytic BOP's with those calculated by matrix diagonalization of the reduced TB Hamiltonian. In the following tables the acronym BOP4 refers to the four-level approximation for the σ bond order which is given by Eqs. (76) and (72) of Paper I, whereas BOP4Z and BOP4S refer to the two variants given by Eqs. (79) and (80), respectively, in which $\delta=\Delta=zero$ [where $\Delta=E_s^H-\frac{1}{2}(E_s^C+E_p^C)$] for BOP4Z together with the *simplification* $b_3=b_1$ for BOP4S. The acronym BOP2S refers to the two-level approximation for the σ bond order, $\Theta^{(2S)}=1/\hat{b}_1$, where the renormalized recursion coefficient $\hat{b}_1$ is evaluated as in Eq. (81) by neglecting the second-order contributions $[h_\pi^{CC}(R_{ik})/h_\sigma^{CC}(R_{ij})]^2$ to the angular function $g_\sigma^C(\theta)$ and by assuming $\delta=\Delta=0$. The acronym BOP2M refers to the two-level approximation for the π bond order, Eq. (101), which was derived using *matrix* recursion in order to guarantee that the expression is independent of the choice of coordinate axes. These analytic BOP results will be compared with the reduced TB values for the realistic situation $\delta\neq\Delta\neq0$ (referred to by the acronym TB) and for the idealized situation $\delta=\Delta=zero$ (referred to by the acronym TBZ).

A. C-H bonds

Table II gives the σ bond orders for the C-H bonds in the hydrocarbon molecules CH_4, C_2H_2, C_2H_4, C_2H_6, C_6H_6, and C_6H_{12} and the hydrocarbon radicals CH_3 and C_2H_5. They have been grouped according to whether they have a local coordination about the carbon atom z of 2 (with bond angles of 180°), 3 (with bond angles around 120°), or 4 (with bond angles around 109°). We see from the last column that as expected, BOP4 provides the exact TB bond orders for the tetrahedral ground state of methane CH_4 and the trigonal ground state of the methyl radical CH_3. Moreover, it is also correct to two decimal places for acetylene C_2H_2. We see that the four-level BOP4 approximation has not yet converged to the exact TB results for the other hydrocarbons with errors of 1.6% for ethane C_2H_6, 1.0% for benzene C_6H_6, and 3.3% for cyclohexane C_6H_{12}. On the other hand, for the idealized situation of $\delta=\Delta=0$, we find from the second last column that BOP4Z reproduces the exact TBZ bond orders to an accuracy of better than 0.7% for all the hydrocarbons considered in the paper. Thus, as expected, the absence of on-site hopping terms in the many-atom diagrams such as Fig. 1 of Paper I leads to a faster convergence of the many-atom BOP expansion than for the case with on-site terms due to $\delta\neq0$ or $\Delta\neq0$.

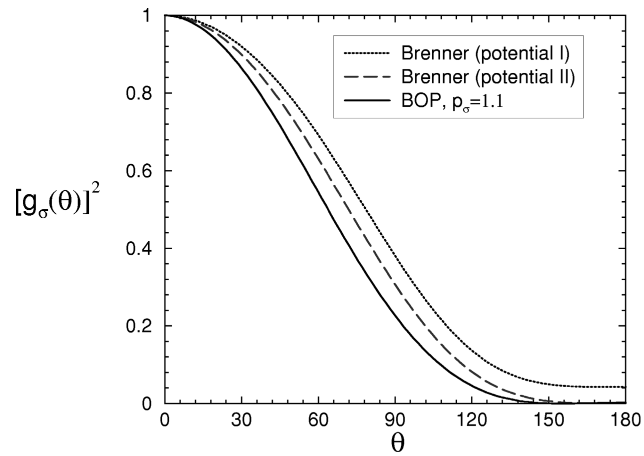

FIG. 1. Comparison of the angular function $g_\sigma^2(\theta)$ predicted by Eq. (82) of Paper I with those of the two empirical Brenner potentials for the hydrocarbons.

The simplified variant, BOP4S, for the σ bond order makes several simplifying assumptions within the idealized situation $\delta=\Delta=0$. First, $\hat{b}_1$ is taken from Eq. (81) of Paper I, in which the second-order π bond contributions with neighboring C atoms have been neglected. For the case of systems with only C-H bonds such as CH_3 and CH_4 this will lead to no errors as can be seen by comparing their BOP4S and BOP4Z $\hat{b}_1$ values in Table II. However, whenever the C-H bond has C neighbors, then small errors will be introduced, the largest being 1% for C_6H_6 in Table II. Second, $\hat{b}_2$ is taken from Eq. (84) of Paper I, again neglecting second-order π bond contributions and also contributions from the second shell of neighbors about the bond. We see from the $\hat{b}_2$ column in Table II that these approximations may lead to errors of up to 4% in $\hat{b}_2$. Fortunately, however, the BOP4S errors in $\hat{b}_1$ and $\hat{b}_2$ tend to work against each other so that the total error introduced into the σ bond order by errors in $\hat{b}_1$ and $\hat{b}_2$ remains below about 1%. Third, $\hat{b}_3$ is taken to be equal to $\hat{b}_1$ within BOP4S in order to avoid the time consuming task of counting all the hopping paths of length six. We see from Table II that this is not a bad approximation for most hydrocarbons, the worst cases being C_2H_2 and C_2H_4

TABLE III. C-C σ bond orders.

System	z	R_0^{CC} (Å)	h_σ^{CC} (eV)	$\hat{b}_1$ BOP4S BOP4Z	$\hat{b}_2$ BOP4S BOP4Z	$\hat{b}_3$ BOP4S BOP4Z	$(b_2/b_1)^2$ BOP4S BOP4Z	Θ_σ^{CC} BOP2S	Θ_σ^{CC} BOP4S	Θ_σ^{CC} BOP4Z TBZ	Θ_σ^{CC} BOP4 TB
C_2	1	1.243	17.843	1.000	0.000	1.000	0.000	1.000	1.000	1.000	0.936
				1.000	0.000	0.000	0.000			1.000	0.936
C_2H_2	3	1.203	19.239	1.000	0.027	1.000	0.001	1.000	1.000	1.000	0.987
				1.000	0.027	0.510	0.001			1.000	0.986
C_2H_4	3	1.339	14.888	1.016	0.216	1.016	0.045	0.984	0.985	0.988	0.962
				1.016	0.216	0.658	0.045			0 .988	0.971
C_6H_6	3	1.390	13.499	1.033	0.349	1.033	0.114	0.967	0.978	0.976	0.947
				1.038	0.371	0.973	0.128			0.979	0.963
C_{gr}	3	1.421	12.705	1.045	0.423	1.045	0.164	0.957	0.975	0.958	0.929
				1.070	0.516	1.031	0.233			0.972	0.957
C_2H_5	3.5	1.498	10.867	1.060	0.473	1.060	0.199	0.943	0.961	0.967	0.931
				1.060	0.473	0.923	0.199			0.969	0.949
C_2H_6	4	1.513	10.529	1.091	0.577	1.091	0.279	0.916	0.939	0.949	0.908
				1.091	0.577	0.913	0.279			0.955	0.936
C_6H_{12}	4	1.536	10.021	1.108	0..640	1.108	0.333	0.902	0.930	0.934	0.868
				1.113	0.654	1.000	0.345			0.945	0.926
$C_\diamond$	4	1.536	10.016	1.128	0.707	1.128	0.392	0.886	0.921	0.914	0.843
				1.143	0.753	1.145	0.434			0.929	0.912

where the assumption that $\hat{b}_3=\hat{b}_1$ leads to errors of 0.4% and 2%, respectively, in the bond order.

The largest total error, therefore, introduced by the simplifying assumptions of $\hat{b}_1$, $\hat{b}_2$, and $\hat{b}_3$ is the 3% error in the bond order for C_6H_6 which is found by comparing the BOP4S and BOP4Z entries in Table II. But, most importantly, comparing BOP4S with the TB values, we see that this simplified four-level variant reproduces the exact TB bond orders to better than 5%. This provides the justification for using BOP4S to model the C-H bond in large scale molecular dynamics simulations.

The grouping in Table II according to local coordination z demonstrates the fact that the C-H bond order decreases with increasing coordination of the C atom, namely, from about 0.99 for $z=2$ through 0.98 for $z=3$ to 0.96 for $z=4$. This weakening of the bond order is reflected in the resultant lengthening of the C-H bond from 1.060 Å in C_2H_2 through 1.087 Å in C_2H_4 to 1.094 Å in C_2H_6. We can understand this trend from the behavior of the normalized recursion coefficient $\hat{b}_1$ which from Eq. (81) of Paper I depends on both the number of neighbors about the bond and the angular function $g_\sigma^C(\theta)$. The angular function is plotted in Fig. 1 for $p_\sigma=1.1$ where we see that it follows closely the angular function of the two empirical Brenner potentials for the hydrocarbons.[3] It is not surprising, therefore, that $\hat{b}_1$ in Table II increases with increasing coordination and decreasing bond angle, since both the number of neighbors summed and the value of the angular function $g_\sigma^C(\theta)$ increase. Hence we find, that the simplified two-level bond order decreases by 7% in going from C_2H_2 to C_6H_{12} down the BOP2S column in Table II. This decrease is countered by the influence of the shape parameter $(b_2/b_1)^2$, so that the decrease is only 3% down the BOP4S column or 4% down the TB column in Table II. Moreover, we find that the inclusion of the shape parameter in BOP4S can enhance the bond order by up to 5%.

B. C-C bonds

Table III gives the σ bond orders for the C-C bonds in the pure carbon systems C_2, diamond and graphite, and the hydrocarbon molecules considered earlier. The C_2 molecule is given the experimental ground-state configuration $\sigma_g^2\sigma_u^2\pi_u^4$. The systems have again been grouped according to the average local coordination about the carbon atoms. We see from the last column that, as expected, BOP4 predicts the exact TB bond order for the four σ states in the C_2 dimer, and provides the bond order for C_2H_2 to within 0.1%. We find that the four-level BOP4 approximation has not yet converged to the exact TB results for the other systems, the single-bonded C-C examples C_2H_6,C_6H_{12} and diamond showing errors of up to 7%. Again, however, the convergence for the idealized situation of $\delta=\Delta=0$ is much faster, the BOP4Z values reproducing the TBZ σ bond orders to better than 1% for all the systems considered. Moreover, the simplified BOP4S values agree with the exact TB bond orders to better than 1.8% for all C-C σ bonds except that of the dimer. This provides the justification for using BOP4S to model the C-C σ bond in large-scale molecular dynamics (MD) simulations of chemical vapor deposition (CVD) diamond growth, for example, since dimers usually play little role in the process as their binding energy of 3.17 eV/atom is far removed from that of other species (see Table I).

Interestingly we see from the last column in Table III that the σ bond order of acetylene C_2H_2 is 5% larger than that of the dimer C_2 even though the former bond has two neighbors whereas the latter has none. This difference in bond order is

TABLE IV. C-C bond orders.

System	z	Θ_σ BOP4S TB	Θ_{π_-} BOP2M TB	Θ_{π_+} BOP2M TB	Θ_{total} BOP TB
C_2	1	1.000	1.000	1.000	3.000
		0.936	1.000	1.000	2.936
C_2H_2	2	1.000	1.000	1.000	3.000
		0.986	1.000	1.000	2.986
C_2H_4	3	0.985	1.000	0.270	2.257
		0.971	1.000	0.137	2.108
C_6H_6	3	0.978	0.707	0.198	1.888
		0.963	0.667	0.107	1.737
C_{gr}	3	0.975	0.577	0.171	1.723
		0.957	0.528	0.094	1.579
C_2H_5	3.5	0.961	0.296	0.203	1.466
		0.949	0.217	0.102	1.268
C_2H_6	4	0.939	0.208	0.208	1.380
		0.936	0.105	0.105	1.146
C_6H_{12}	4	0.930	0.197	0.188	1.350
		0.926	0.101	0.101	1.128
$C_\diamond$	4	0.921	0.177	0.177	1.302
		0.912	0.103	0.103	1.118

reflected in the values of the residues w_n that enter the BOP4 expression, Eq. (78), in Paper I. We find for acetylene that $w_1=0.4756$, $w_2=0.0172$, $w_3=-0.026$, $w_4=-0.4669$ whereas for the dimer $w_1=0.4835$, $w_2=-0.0154$, $w_3=0.0165$, $w_4=-0.4846$. Thus, the bond order $2(w_1+w_2)$ takes the value 0.986 for acetylene but 0.936 for the dimer. This increased bond order in acetylene compared to the dimer is reflected in the decreased experimental equilibrium bond length of 1.206 Å compared to 1.240 Å. A further consequence of this behavior in the residues for the dimer is that N_2 will be more strongly bound than C_2 because the third σ eigenstate will now be doubly occupied and contribute the additional attractive energy $4w_3h_\sigma^{NN}$ to the bond. For $h_\sigma^{NN}=20$ eV we find an extra 1.2 eV of cohesion.

Table IV compares the π bond orders predicted by BOP2M with those evaluated by TB. We see that the conventional *saturated* π bonds in C_2, C_2H_2, and C_2H_4 are recovered by the two-level matrix recursion. Moreover, we see that the *conjugated* π bonds in benzene and graphite are also reproduced to within 10%. In fact, it follows from Eqs. (97)–(101) of Paper I that the π bond order for benzene and graphite can be written

$$\Theta_{ij,\pi}^{(2M)}=\Theta_{ij,\pi_-}^{(2M)}+\Theta_{ij,\pi_+}^{(2M)}$$
$$=z_c^{-1/2}+2\left\{3+z_c+3\left(\frac{p_\sigma}{p_\sigma+1}\right)\sum_{k\neq j}[\hat{h}_\sigma^{C\kappa}(R_{ik})]^2\right\}^{-1/2}, \tag{4}$$

where z_c is the number of the nearest-neighbor carbon atoms about a given carbon site. Thus the conjugated contribution to the π bond order in benzene and graphite takes the values $1/\sqrt{2}$ and $1/\sqrt{3}$, respectively, within the BOP2M approximation. We should note that BOP4 would have predicted the exact TB value of 2/3 for the conjugated π bond in benzene because this is a four-level system (see Fig. 1.7 of Ref. 10). However, this would only have been true for the particular choice of one of the coordinate axes being normal to the plane of the benzene ring. BOP2M, on the other hand, is independent of the choice of axes which is, of course, central to any meaningful interatomic potential. The *unsaturated* π bonds in Table IV are not so well reproduced by the two-level matrix approximation, which leads to most of the errors associated with the analytic BOP treatment of the C-C bonds as we will see in the next section.

Finally, in Table IV we compare the total C-C bond orders predicted by BOP with those evaluated by TB. We see that BOP provides a quantitative treatment of the valence bond concept of single, double, triple, and conjugated π bonds. Moreover, as stressed in Sec. V of Paper I, BOP provides the first interatomic potential that correctly describes the breaking of saturated bonds on radical formation such as, for example, in going from C_2H_4 to C_2H_5 in the π_- column of Table IV. Thus, the analytic BOP's are based on a formalism that overcomes the inherent problems of the Tersoff potential with its overbinding of radicals and poor handling of conjugation.

IV. BINDING ENERGIES

In this section we compare the binding energies predicted by the analytic BOP's with those evaluated within the reduced TB model. Table V presents the results for the pure carbon systems C_2, graphite and diamond at the experimental equilibrium bond lengths. The dimer has been given the experimental ground-state configuration $\sigma_g^2\sigma_u^2\pi_u^4$. We see that BOP4S reproduces the σ bond energy of graphite and diamond to within 0.4 eV per C-C bond, whereas the error in the dimer is five times larger due to the 6% error in the bond

TABLE V. Binding energies of pure carbon systems.

System	h_σ^{CC} (eV)	Θ_σ^{CC} BOP4S TB	U_σ (eV/bond) BOP4S TB	h_π^{CC} (eV)	Θ_π^{CC} BOP2M TB	U_π(eV/bond) BOP2M TB	No of bonds (per atom)	U_{rep} (eV/atom)	U_{prom}(eV/atom) BOP TB	U(eV/atom) BOP TB
C_2	17.843	1.000	−35.686	2.761	2.000	−11.046	0.5	15.507	5.946	−1.913
		0.936	−33.411		2.000	−11.046			4.352	−2.369
C_{gr}	12.705	0.975	−24.749	1.966	0.748	−2.942	1.5	27.129	5.648	−8.759
		0.957	−24.316		0.622	−2.446			5.652	−7.360
$C_\diamond$	10.016	0.921	−18.448	1.550	0.355	−1.100	2	25.214	5.376	−8.506
		0.912	−18.268		0.206	−0.638			5.370	−7.235

TABLE VI. Hydrocarbon bond energies.

System	z^C	h_σ^{CC} (eV)	Θ_σ^{CC} BOP4S TB	U_σ^{CC}(eV/bond) BOP4S TB	h_π^{CC} (eV)	Θ_π^{CC} BOP2M TB	U_π^{CC}(eV/bond) BOP2M TB	h_σ^{CH} (eV)	Θ_σ^{CH} BOP4S	U_σ^{CH}(eV/bond) BOP4S TB
C_2H_2	2	19.239	1.000	−38.467	2.977	2.000	−11.910	9.818	1.003	−19.705
			0.986	−37.958		2.000	−11.910		0.993	−19.492
CH_3	3	—	—	—	—	—	—	9.491	0.990	−18.785
									0.977	−18.545
C_2H_4	3	14.888	0.985	−29.323	2.304	1.270	−5.854	9.377	1.006	−18.858
			0.971	−28.925		1.137	−5.240		0.973	−18.545
$C_2H_5^{(1)}$	3	10.867	0.961	− 20.886	1.682	0.499	−1.679	9.556	0.991	−18.938
			0.949	−20.626		0.319	−1.074		0.975	−18.632
C_6H_6	3	13.499	0.978	−26.401	2.089	0 .905	− 3.780	9.393	1.010	−18.971
			0.963	−25.991		0.774	−3.234		0.972	−18.253
CH_4	4	—	—	—	—	—	—	9.377	0.973	−18.243
									0.962	−18.050
$C_2H_5^{(2)}$	4	10.867	0.961	− 20.886	1.682	0.499	−1.679	9.393	0.973	−18.273
			0.949	− 20.626		0.320	−1.074		0.956	−17.951
$C_2H_5^{(3)}$	4	10.867	0.961	− 20.886	1.682	0.499	−1.679	9.328	0.972	−18.137
			0.949	−20.688		0.320	−1.074		0.947	−17.668
C_2H_6	4	10.529	0.939	−19.765	1.629	0.416	−1.357	9.263	0.973	−18.020
			0.936	−19.719		0.210	−0.685		0.958	−17.747
$C_6H_{12}^{(1)}$	4	10.021	0.931	−18.649	1.551	0.385	−1.195	9.118	0.974	−17.755
			0.926	−18.559		0.202	−0.626		0.955	−17.425
$C_6H_{12}^{(2)}$	4	10.021	0.931	−18.649	1.551	0.385	−1.195	9.078	0.971	−17.630
			0.926	−18.559		0.202	−0.626		0.954	−17.311

order. BOP2M, on the other hand, reproduces the π bond energy to within 0.5 eV per C-C bond for graphite and diamond with no error for the dimer. We find that the π bond energy contributes 25%, 9%, and 3% to the total bond energies of the dimer, graphite, and diamond, respectively. The simple expression for the promotion energy, Eq. (108) of Paper I, reproduces the promotion energy to better than 0.03 eV per carbon atom for graphite and diamond, but with the much larger error of 1.54 eV for the dimer as expected from comparing Eq. (108) with Eq. (44) in Paper I. The total errors in the binding energy, therefore, lead to overbinding of up to 0.9 eV per C-C bond in diamond and graphite. The

TABLE VII. Hydrocarbon total binding energies.

System	z	$U_{\text{bond}}^{\text{CC}}$(eV) BOP4S TB	$U_{\text{bond}}^{\text{CH}}$(eV) BOP4S TB	U_{bond}^{tot}(eV) BOP4S TB	U_{rep}(eV)	U_{prom} (eV) BOP4S TB	U_{bind}^{tot} (eV) BOP4S TB
C_2H_2	2	− 50.377	−39.410	−89.787	60.690	11.643	−17.454
		−49.868	−38.984	−88.852		11.852	−16.310
CH_3	3	—	−56.355	−56.355	37.847	5.305	−13.203
			−55.635	−55.635		5.291	−12.497
C_2H_4	3	−35.177	−75.432	−110.609	72.454	10.611	−27.544
		−34.165	−72.972	−107.137		10.980	−23.703
C_6H_6	3	−181.086	−113.826	−294.912	193.237	33.552	−68.123
		−175.344	−109.518	−284.860		33.476	−58.148
C_2H_5	3.5	−22.565	−92.559	−115.124	76.753	10.718	−27.653
		−21.700	−90.834	−112.534		10.673	−25.108
CH_4	4	—	−72.972	−72.972	49.317	5.289	−18.366
			−72.200	−72.200		5.294	−17.589
C_2H_6	4	−21.122	− 108.12	−129.242	86.258	10.640	−32.344
		−20.404	−106.482	−126.886		10.635	−29.993
C_6H_{12}	4	−119.064	−212.31	−331.374	217.243	31.898	−82.233
		−115.110	−208.348	−323.458		31.841	−74.374

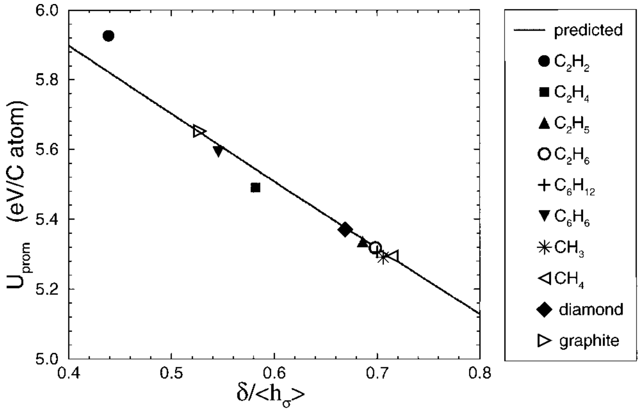

FIG. 2. Comparison of the promotion energy predicted by the simple analytic BOP expression, Eq. (108) of Paper I, with the exact TB value for particular hydrocarbon molecules and graphite and diamond.

errors in the dimer work against each other to also leave a total error of 0.9 eV per C-C bond.

Table VI compares the hydrocarbon bond energies evaluated by BOP and reduced TB. We see that the errors in the C-H bond energies are less than 0.7 eV per bond. The errors in the C-C σ and π bond energies are comparable, both being less than 0.7 eV per bond, but with the total error better than 0.9 eV per C-C bond. Table VII compares the hydrocarbon binding energies. We see that the errors in the promotion energy are less than 0.18 eV per carbon atom for all the molecules. This good agreement is illustrated in Fig. 2, where we find that the TB values for the promotion energy fall very close to the predicted curve. It follows from the last column in Table VII that the total error leads to an overbinding in the hydrocarbons by up to 0.9 eV per bond.

The total error made by BOP in treating the C-H and C-C bonds, namely 0.9 eV per bond, is comparable to the errors made by conventional TB as compared to experiment in Table I. We should note, however, that the overbinding of the C-C bond energy within BOP is primarily due to the increased bond order of the unsaturated π bond that is predicted by BOP2M. If the analytic BOP's were to be fitted directly to experiment rather than use the values of the original TB parameters, then this overbinding of the π bond could be countered by treating $\hat{h}_\sigma$ that enters the bond order BOP2M [see, for example, Eq. (4)] as a fitting parameter which is independent of the bond integrals h_σ and h_π that enter the binding energy, Eq. (2). This fitting of $\hat{h}_\sigma$ would leave both the saturated and conjugate π bond contributions unaltered. The fitting of the analytic BOP's to experiment and their application in large-scale MD simulations of CVD diamond growth is currently ongoing research.

V. CONCLUSIONS

We have studied the accuracy of the analytic bond-order potentials for the hydrocarbons that were derived within the TB model in Paper I. We have found that the inclusion of the shape parameter $(b_2/b_1)^2$ in BOP4S can lead to an increase in the bond order by up to 5%. This corresponds to an increase in binding energy of about 0.5 eV per bond. We have shown that BOP2M provides a good description of saturated and conjugate π bonds in carbon systems. Moreover, it is the first interatomic potential that handles correctly the breaking of saturated π bonds on radical formation. This overcomes a major deficiency of the Tersoff potential and avoids the many additional *ad hoc* parameters in the Brenner potential. The analytic BOP's were found to reproduce the TB values for the C-H and C-C bond energies to better than 0.9 eV per bond. This error is comparable to that made by the original TB model compared to experiment.

Several further challenges remain for future research. First, spin polarization must be included within the BOP framework in order to handle radicals such as CH and CH_2. Second, the constraint of local charge neutrality will need to be relaxed and ionic interactions treated explicitly for most other covalent systems of interest. Thirdly, the simple analytic expression for the promotion energy might have to be generalized to include changes in bond angles as well as bond lengths about the ground state before transverse vibrational modes are predicted accurately. Finally, the most difficult challenge of all will be to extend the analytic BOP's and the TB model to handle activation barriers reliably, perhaps through the introduction of environmentally dependent repulsive potentials and bond integrals.[11,12]

ACKNOWLEDGMENTS

We gratefully acknowledge the support of the Defense Advanced Research Projects Agency and the Naval Research Laboratory under Contract No. N00014-97-1-G015 on ''The development of analytic bond-order potentials for atomistic simulations in vapor processing.'' The project was managed by Dr. Jim Butler who provided many insightful comments on diamond growth. The OXON code was used to calculate TB properties. The computations were performed with the use of the computer facilities in the Materials Modelling Laboratory at the Department of Materials, University of Oxford.

[1] D.G. Pettifor and I.I. Oleinik, preceding paper, Phys. Rev. B **59**, 8487 (1999).

[2] A.P. Horsfield, P.D. Godwin, D.G. Pettifor, and A.P. Sutton, Phys. Rev. B **54**, 15 773 (1996); **54**, 15 776 (1996); P.D. Godwin, A.P. Horsfield, A.M. Stoneham, S.J. Bull, I.J. Ford, A.H. Harker, D.G. Pettifor, and A.P. Sutton, *ibid.* **54**, 15 785 (1996).

[3] D.W. Brenner, Phys. Rev. B **42**, 9458 (1990).

[4] J. Tersoff, Phys. Rev. Lett. **56**, 632 (1986); Phys. Rev. B **37**, 6991 (1988); Phys. Rev. Lett. **61**, 2879 (1988); Phys. Rev. B **39**, 5566 (1989).

[5] C.H. Xu, C.Z. Wang, C.T. Chan, and K.M. Ho, J. Phys.: Condens. Matter **4**, 6047 (1992).

[6] B.N. Davidson and W.E. Pickett, Phys. Rev. B **49**, 11 253 (1994).

[7] L. Goodwin, A.J. Skinner, and D.G. Pettifor, Europhys. Lett. **9**, 701 (1989).

[8] J.C. Slater and G.F. Koster, Phys. Rev. **94**, 1468 (1954).
[9] D.G. Pettifor, *Bonding and Structure of Molecules and Solids* (Clarendon Press, Oxford, 1995).
[10] J.K. Burdett, *Chemical Bonding in Solids* (Oxford University Press, New York, 1995).
[11] M.S. Tang, C.Z. Wang, C.T. Chaen, and K.M. Ho, Phys. Rev. B **53**, 979 (1996).
[12] D. Nguyen-Manh, D.G. Pettifor, S. Znam, and V. Vitek, in *Tight-Binding Approach to Computational Materials Science*, edited by P.E.A. Turchi, A. Gonis, and L. Colombo, MRS Symposia Proceedings No. 491 (Materials Research Society, Pittsburgh, 1998), p. 353.